Accepted for presentation in: IEEE International Conference on Communications Workshops (ICC Workshops): The IEEE International Workshop on Communication, Computing, and Networking in Cyber Physical Systems (CCNCPS), Kansas City, USA, Mai 2018.

Enhanced UAV Indoor Navigation through SLAM-Augmented UWB Localization

Janis Tiemann*, Andrew Ramsey† and Christian Wietfeld*
*TU Dortmund University, Communication Networks Institute (CNI)
{janis.tiemann, christian.wietfeld}@tu-dortmund.de
†Rochester Institute of Technology (RIT)
{axr8451}@rit.edu

***Abstract*—Applications using low cost quadrotor solutions find broad attention in both research and industry. While autonomous flight in outdoor environments is achieved using global navigation satellite systems, dedicated precise wireless localization is a promising candidate to enable indoor navigation. However, equipping large industrial areas with wireless localization is possible, but providing the required coverage may not be economical. Therefore, this work aims to augment and fuse state of the art ultra-wideband localization with monocular simultaneous localization and mapping to enable autonomous flight in areas not covered by wireless localization. For the in-depth validation of the proposed approach, two experiments are performed: the first one is providing an extensive experimental analysis of the accuracy of different localization methods for drones, whereas the second experiment is showing that precise waypoint flight in areas not covered by wireless localization is feasible, lowering the threshold for integration of future drone-based cyber physical systems in current industrial environments.**

***Keywords*—Cyber Physical Systems, Industrial Applications, Ultra-wideband (UWB), Wireless Positioning, Unmanned Aerial Vehicle (UAV), Simultaneous Localization and Mapping (SLAM).**

I. Introduction and Related Work

Integrating highly mobile sensor and actor platforms into future cyber-physical systems for productive applications is a long-term goal of current efforts in research and industry. Due to the ongoing trends in miniaturization and advances in control low cost quadrotor and unmanned aerial vehicles (UAV) solutions gained significant attention over the past years. For autonomous operation however, either global navigation satellite systems (GNSS) in outdoor environments or expensive optical motion capture systems in indoor environments are required [1]–[3]. Recently, low-cost wireless localization has also begun to enable autonomous UAV indoor navigation [4], [5]. Therefore, this work aims to solve two problems of current indoor drone navigation. The first problem is the range and coverage cost limitations of wireless localization. The second goal is to provide absolute orientation needed for UAV control in environments where inertial measurement-based odometry fails to provide reliable feedback. To overcome those limitations, this work aims to use the already in-place camera of the UAV to augment and fuse state of the art ultra-wideband (UWB) wireless localization with the visually obtained information. The concept of leveraging monocular or stereoscopic visual data is not new and there are many approaches starting from visual odometry based on optical flow [6], [7] to simultaneous localization and mapping (SLAM) [8]. Monocular SLAM is chosen for the proposed approach as it can be added to existing setups using low-cost drones with no additional components. In comparison to [9]–[12] no laser scanner, laser grid or radar sensors are needed. However, in contrast to binocular methods [13] or laser-based mapping, monocular SLAM is not capable of providing absolute scale and global reference for autonomous indoor navigation. However, high precision navigation solely based on monocular information is not possible as it suffers from inaccuracies and scaling uncertainties. There are approaches for scale-free exploration using monocular SLAM such as [14]. The usage of optical flow sensors to obtain the scale of the estimation is presented in [15]. Mostly though, the altitude, either through an ultrasonic sensor or a barometer, is used to estimate the scale, see [16]–[18]. The problems with most approaches is, they do not provide absolute reference and lack the capabilitiy of autonomous waypoint flight to globally specified positions. A comparative listing of scaling and referencing methods is provided in Tab. I.

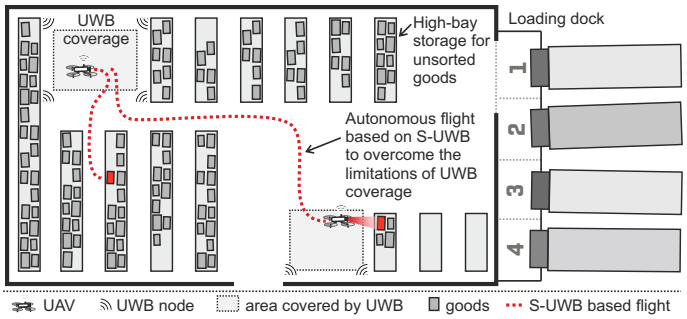

Fig. 1. Illustration of an industrial application for UAV indoor navigation. The autonomous UAVs are used for stocktaking and tracking of goods. The proposed method overcomes the coverage limitations of wireless localization.

To enable practical deployment in future cyber physical industrial contexts, this work proposes SLAM-augmented UWB localization (S-UWB) to enable autonomous flight in- and between areas not covered by wireless indoor localization systems, see Fig. 1. To prove the capabilities of the proposed approach a detailed experimental evaluation in a practical industrial setup is conducted. Since the presented approach requires a highly networked architecture and frequent information exchange to control the individual UAVs in a larger deployment, a scalability analysis of the wireless network requirements is conducted for different potential S-UWB configurations. A video along with the raw data of the aforementioned experiments is provided alongside this work.

II. Proposed System Implementation

In order to control unmanned aerial vehicles indoors the on-board GNSS-optimized control has to be replaced. In this work, a cascaded control loop is employed. This control loop requires position, velocity and orientation feedback to properly control the UAV. While the wireless localization can deliver absolute position information within its coverage, the velocity is determined using the on-board optical flow sensor. A transformation from the local UAV coordinates into the global frame is needed to properly rotate the optical flow information back into the globally referenced control loop. The same applies for the control loop output. Hence, accurate absolute and long-term stable orientation information is required for a successful indoor flight.

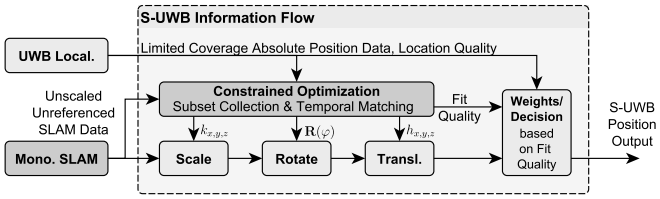

Fig. 2. Block diagram of the S-UWB concept. The UWB and SLAM data is sampled, temporally matched and fitted using optimization. Based on the quality of the results the S-UWB position output is enabled.

Modern accurate wireless localization is usually based on ultra-wideband communication systems. However, the transmission power and therefore the range of such systems has regulatory limitations due to the very high bandwidth required for precise time-of-arrival (TOA) estimation of the received packets. Another aspect are non-line-of-sight (NLOS) conditions through obstacles in the operation area of the wireless location system such as in a high-bay storage. While many communication systems can operate within NLOS conditions, the introduced propagation delay can lead to severe errors in the UWB location estimation. Therefore, the goal of the proposed approach is to enable autonomous flight outside the wireless location system's area of safe operation.

A. Proposed Approach: SLAM Augmented UWB (S-UWB)

The proposed approach augments the UWB localization information with data from a monocular SLAM system. In order to provide this capability, the data from the UWB and SLAM has to be matched to operate in the same context. The SLAM based postion estimation is without a global reference, scale or orientation. This approach proposes the use of UWB location information to estimate those unknowns through optimization, see Fig. 2. The samples of the UWB localization $f_{u,i}$ and the monocular SLAM $f_{s,i}$ are recorded and temporally matched for discrete timesteps i. A multi-step regression, estimating the scale factor vector $\mathbf{k} = (k_x, k_y, k_z)^T$, translatory offsets

TABLE I. Comparison of Monocular SLAM Scaling Sources

method	accuracy	abs. position	start point ind.	overhead	terrain
odometry	o	-	-	+	+
barometer	o	-	-	+	+
ultrasonic	+	-	-	+	-
feature-based	+	+	o	-	+
prop. approach	+	+	+	o (-)*	+

*UWB system not already in place

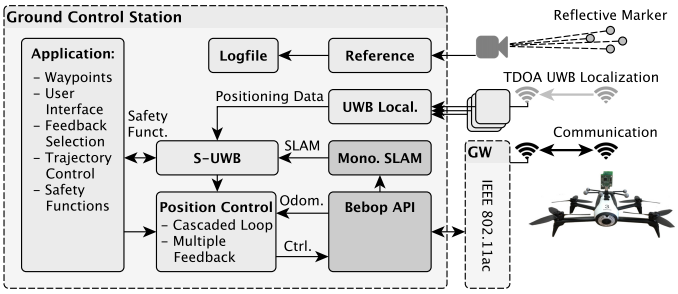

Fig. 3. Block diagram of the system topology of the experimental setup. Note that the reference system is not needed for UWB-based or S-UWB based control but may be used as control feedback for comparison.

$\mathbf{h} = (h_x, h_y, h_z)^T$ and the rotational offset φ is employed using the Levenberg-Marquardt algorithm, see (1) and (2).

$$\underset{\varphi,\mathbf{h},\mathbf{k}}{\arg\min} \|F(\varphi, \mathbf{h}, \mathbf{k})\|_2^2 \tag{1}$$

$$F(\varphi, \mathbf{h}, \mathbf{k}) = (f_{s,i}(\varphi, \mathbf{h}, \mathbf{k}) - f_{u,i})_{i=1,\dots,m} \tag{2}$$

In order for the optimization to work properly, a subset of m samples with a certain spatial spread has to be collected. Therefore, an initialization phase is required before S-UWB is capable of estimating the correct scale, translatory and rotational parameters. In the course of this work, a predefined trajectory is used to acquire sufficient spatial spread to fit the UWB localization and the monocular SLAM estimate. After completion of this trajectory the optimization is conducted. Note that estimation of the rotational components was not part of the experiments as a static initialization direction was chosen. As a safety measure, the residuals of the optimization were used to assess the fit quality and reject potential outliers. Upon rejection re-initialization enables fault-tolerant operation of the system.

B. Experimental Testbed

In order to enable a flexible development environment while maintaining the option to quantify the achieved results, a complex experimental testbed was designed. A block diagram of the system topology is depicted in Fig. 3. The *Parrot Bebop 2*, a highly integrated low-cost drone serves as the test platform. All positioning, visual computation and control are handled by the groundstation. The individual components are interfaced using the Robot Operating System (ROS) [19] as it provides a significant set of interfaces like the ROS driver for the Bebop drones developed by Monajjemi et al., see [20]. An *OptiTrack* motion capture system with a set of eight cameras is used as a ground-truth in a truss-cage to obtain the localization error of the UWB system and the S-UWB estimation. The monocular SLAM component used in this work is ORB-SLAM, a recent SLAM system for

TABLE II. UWB Anchor Positions used in the Experiments.

anchor	sync	1	2	3	4	5	6	7	8
x [m]	-2.31	-2.31	-2.31	-2.23	-2.23	2.20	2.20	2.30	2.30
y [m]	2.19	2.19	2.19	-2.28	-2.28	-2.27	-2.27	2.20	2.20
z [m]	1.2	0.90	2.90	0.90	2.90	0.90	2.90	0.90	2.90

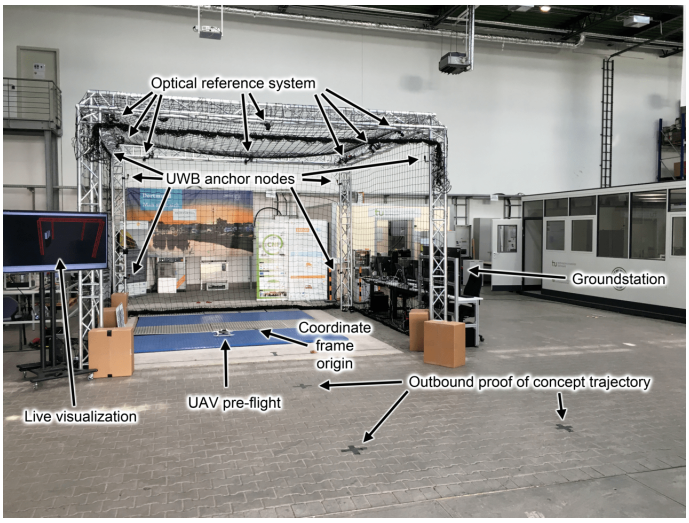

Fig. 4. Photo of the experimental setup in an industrial environment. The area inside the truss cage is covered by an optical reference system and wireless localization. Outside the cage S-UWB is used for navigation.

monocular [21], stereo and RGB-D cameras [22] developed by Mur-Artal et. al. Depending on the required use-case and computational capabilities, other SLAM systems might be used in combination with the proposed approach through the standardized ROS interface. The wireless localization is based on the ATLAS UWB positioning system developed by the authors of this work [23]. The system was modified to handle all relevant communication over ROS. It should be noted that the system is based on the time-difference of arrival (TDOA) of the packets broadcasted by a UWB transceiver mounted on the UAV. Using the TDOAs enables the system to provide position updated for a multitude of mobile users while being energy efficient. Here, the approximate update rate of the position is 32 Hz with a random component to avoid interference. Due to strong reflections from the metal ground plate of this specific experimental setup, the system was calibrated with a vertical offset to account for the resulting positioning error.

III. Experimental Evaluation

In order to evaluate the capabilities of the proposed system, two different experiments were conducted. The experimental setup is depicted in Fig. 4. The first experiment focused on error quantification and was therefore placed within the coverage of the previously described optical reference system inside the truss-cage. The second experiment involved a proof of concept flight, outside of the controlled environment, to show that the proposed approach enables flights between areas covered by wireless localization as described in section I. We also provide the raw experimental logging files of the described experiments [24] and a video [25].

TABLE III. Waypoints of the Quantification Experiment

waypoint	1	2	3	4	5	6	7	8	9	10
x [m]	0.00	0.00	0.00	0.00	1.40	1.40	-1.40	-1.40	1.40	1.40
y [m]	0.00	0.00	0.00	0.00	0.00	-1.40	-1.40	1.40	1.40	0.00
z [m]	1.00	1.90	0.50	1.00	1.00	1.00	1.00	1.00	1.00	1.00
φ [°]	$\pi/2$	$\pi/2$	$\pi/2$	$\pi/2$	$\pi/2$	π	$-\pi/2$	0	$\pi/2$	π
waypoint	11	12	13	14	15	16	17	18	19	20
x [m]	0.00	0.00	1.40	0.00	-1.40	0.00	1.40	0.00	0.00	0.00
y [m]	0.00	0.00	0.00	-1.40	0.00	1.40	0.00	0.00	0.00	0.00
z [m]	1.00	1.50	1.50	1.50	1.50	1.50	1.50	1.50	1.00	0.00
φ [°]	$-\pi/2$	$\pi/2$	$\pi/2$	$3\pi/4$	$-3\pi/4$	$-\pi/4$	$\pi/4$	$-\pi/2$	π	$\pi/2$

A. Experimental Accuracy Analysis

To evaluate and quantify the capabilities of the S-UWB approach in contrast to the UWB and reference systems, a complex trajectory inside the truss cage was used. To achieve statistical relevance and explore the limits of the S-UWB approach, three different patterns were flown. After lift-off in the center, a square was flown with the camera facing in the direction of movement. The first iteration of this square was used for initialization of the S-UWB system. After the initialization, the square movement was repeated three times. The drone then flew to the center, ascended while rotating 180° and flew in a diamond pattern with the camera facing outwards three times. Finally, the camera of the drone was set to track the center of the cage and the diamond pattern was once again flown three times. A list of the waypoints and orientations is given in Tab. III without the repetitions. In order to analyze the performance in different modes of operation, three different experiments were conducted:

- **Reference-based**: control based on motion capture system for position, velocity and yaw feedback
- **UWB-based**: control through UWB for position feedback, odometry for velocity and altimeter for height
- **S-UWB-based**: initial control through UWB and altimeter, after initialization S-UWB-based position feedback and odometry-based velocity feedback.

A time-series of the resulting trajectories for the S-UWB based flight is given in Fig. 6. The individual components of the position estimation of all relevant localization systems are depicted next to the yaw error for the orientation estimation. Fig. 6 is divided in four sections. The first part depicts the initial phase where positioning data from the UWB system was gathered. During this time period, the altimeter was used to gather height information in the z axis. Based on the gathered data, initial S-UWB parameters were calculated as described in section II-A at the intersection between part one and part two. After successful estimation of the coefficients, S-UWB tracked the true trajectory quite well, as measured by ground-truth. It is also clearly visible that the UWB system had a small error in its tracking of the drone. The odometry however, suffered

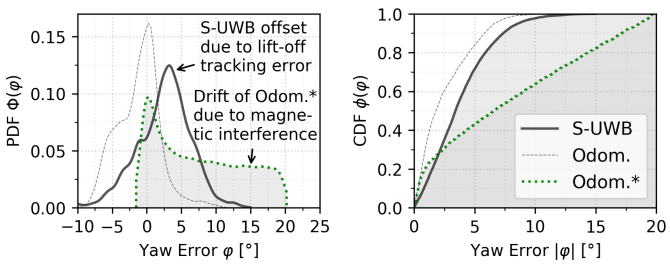

Fig. 5. Normed probability distribution function $\Phi(\varphi)$ and cumulative distribution function $\phi(\varphi)$ of the yaw error φ. Note the difference between the SLAM-based yaw, the odometry estimation in an environment with few magnetic disturbances (Odom.) and the yaw estimation in an area with inconsistent magnetometer readings (Odom.*) as observed in [5].

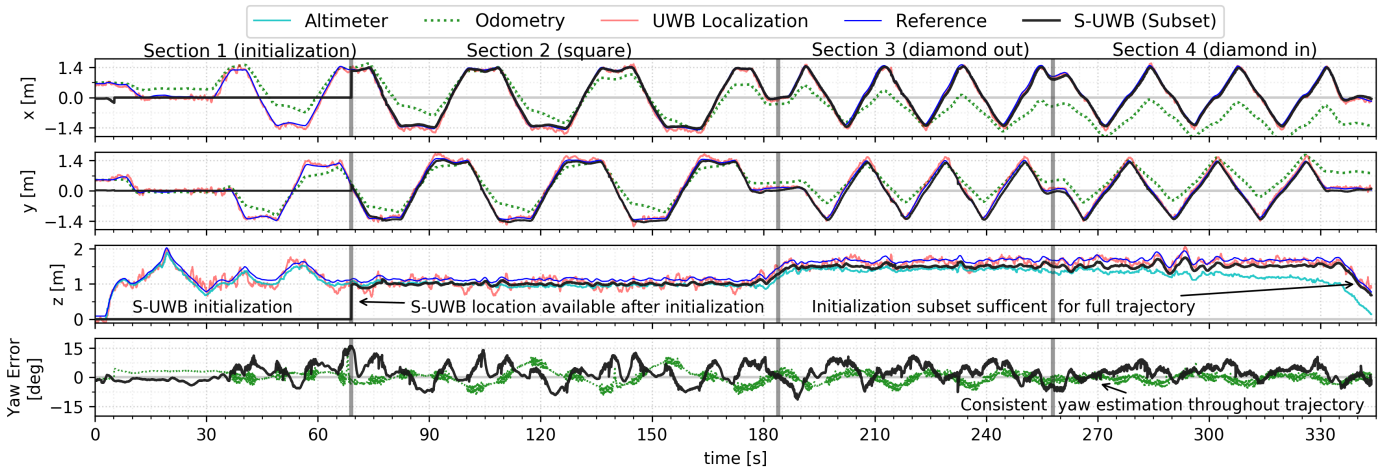

Fig. 6. Timeseries of the quantification experiment. Note the difference between different approaches such as the UWB-based localization, odometry and S-UWB. Reference-based control was chosen to enable fair comparison of the individual localization results. Note the long-term drift of the odometry.

from long-term drift in both x and y. Along the vertical axis the altimeter mostly matched the ground-truth but was subject to some long-term drift as well. The wireless localization system was also able to resolve the height of drone, but with more noise than the altimeter. In contrast, the S-UWB system did not suffer from long-term drift like the altimeter and was less noisy than the wireless localization.

Since one goal of the proposed system is to eliminate the orientation estimation problem in areas where magnetometer readings are disturbed, Fig. 5 provides a statistical analysis of the yaw error estimated by S-UWB and odometry systems. The experiment was conducted in an area with few magnetic interferences. However, to prove the necessity of the proposed method, the yaw error from [5] is also shown as an example for areas with inconsistent magnetometer readings. Due to the fast movement during lift-off and the corresponding higher tracking error, a repeatable offset is introduced to the SLAM based yaw estimation. It should be noted that in order to provide a broader statistical relevance, the yaw data of all three flights was used for the error analysis.

To assess the capabilities of the different localization approaches, a detailed statistical analysis of the reference-based flight is given in Fig. 7. The optimum achievable results S-UWB (Full) were found by fusing the SLAM values to the reference system using the entire flight duration, not just the initialization period as the partial trajectory readings S-UWB (Subset) used for S-UWB based control feedback. The location estimation is shown alongside the UWB-based localization results and the odometry estimation. It is clearly visible that the odometry cannot be relied upon as a source of navigation data for any axis. Along the vertical axis, S-UWB performs quite well, with a 75 % quantile error of 5.9 cm, only 3.7 cm larger than the theoretical best. In the horizontal plane, it has a third quartile error of 22.5 cm. When the z-axis error is also taken into account, a 0.7 cm increase in the third quartile error for S-UWB is seen, as compared to 5.0 cm for the UWB and 0.2 cm for the full trajectory case. Another measure of the quality of the control system is how much the drone did deviate from the planned flight path. Fig. 8 shows the error

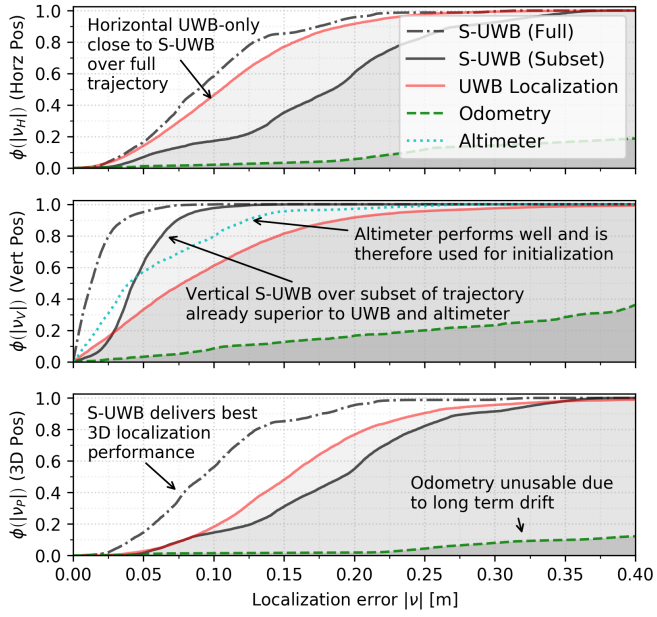

Fig. 7. Cumulative distribution functions of the absolute localization error along the vertical axis $|\nu_V|$, the horizontal plane $|\nu_H|$ and the 3D space $|\nu_P|$. The results cover multiple systems: the wireless UWB localization, the partial trajectory S-UWB (Subset) estimation used during the flights, the full trajectory S-UWB (Full) estimation and the odometry.

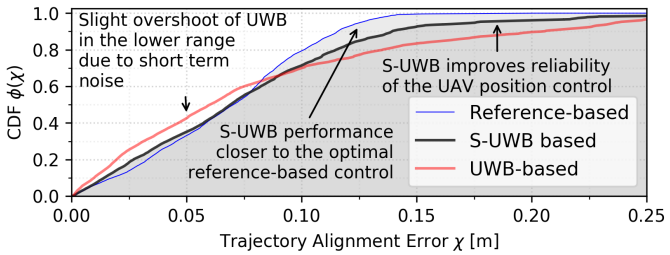

Fig. 8. Cumulative distribution function of the trajectory alignment error $|\chi|$. Note that the proposed S-UWB based control only using the initialization phase is better than the UWB-based control. This is caused through the higher short-term noise of the wireless localization compared to S-UWB.

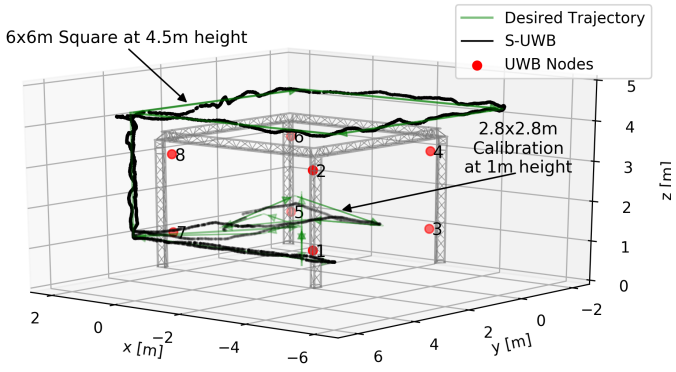

Fig. 9. Trajectory of the proof of concept flight. Note that the UAV is flying outside the wireless localization system's safe area of operation. The control loop of the UAV is solely relying on the S-UWB estimation outside the cage.

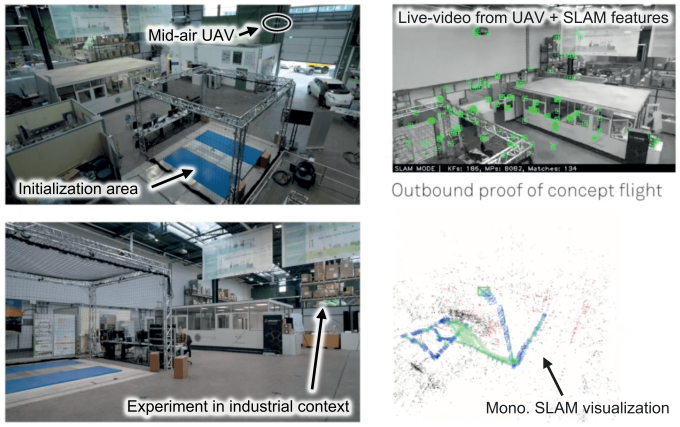

Fig. 10. Still of the video provided alongside this work [25]. The UAV is flying outside the truss-cage to prove the viability of the proposed method.

between the expected and actual paths of travel for each of the experiments performed. Because the short-term height control is drone-based, the controller has little influence over the immediate altitude. Thus, only errors in the horizontal plane were considered. The UWB localization has a 90 % quantile error of 20.5 cm, followed by the augmented S-UWB system at 13.9 cm, and finally the reference motion capture system at 11.5 cm. The small spread shows that the S-UWB system is capable of providing positioning data to the control system that allows for effective navigation of the drone in the environment.

B. Flying Outside the Box: Experimental Proof of Concept

To qualitatively determine the suitability of the system for longer flights without the UWB or motion capture system, a proof of concept flight was performed. The UAV starts with height initialization and a UWB controlled square similar to section III-A. After the square is complete and the coefficients are initially estimated another square is flown based on S-UWB control to ensure proper operation. Here, automatic safety margins were deployed and a safety landing is performed if the S-UWB estimation deviated too much from the UWB. Once the second square was successful, the UAV leaves the cage, turns, and flies along the outbound proof of concept trajectory as depicted in Fig. 4. After a 6 m lateral movement facing in direction of flight, the UAV flies the same way back and initiates an ascend to 4.5 m to start a 6 m × 6 m square above the truss-cage. A complete list of waypoints is given in Tab. IV. The total length of the path, flown using S-UWB, was 62.67 m. The three dimensional trajectory recorded through S-UWB is depicted in Fig. 9. It can be clearly seen that the UAV is capable of following the predefined trajectory in a repeatable

TABLE IV. WAYPOINTS OF THE PROOF OF CONCEPT EXPERIMENT

waypoint	1	2	3	4	5	6	7	8	9	10	11
x [m]	0.00	0.00	0.00	0.00	0.00	1.40	1.40	-1.40	-1.40	0.00	0.00
y [m]	0.00	0.00	0.00	0.00	1.40	1.40	-1.40	-1.40	1.40	1.40	6.00
z [m]	1.00	1.90	0.50	1.00	1.50	1.00	1.50	1.00	1.50	1.00	1.50
φ [°]	$\pi/2$	$\pi/2$	$\pi/2$	$\pi/2$	0	$\pi/2$	π	$-\pi/2$	0	$\pi/2$	0
waypoint	12	13	14	15	16	17	18	19	20	21	22
x [m]	-6.00	-2.00	0.00	0.00	0.00	-6.00	-6.00	0.00	0.00	0.00	0.00
y [m]	6.00	6.00	6.00	6.00	0.00	0.00	6.00	6.00	6.00	0.00	0.00
z [m]	1.50	1.50	1.50	4.50	4.50	4.50	4.50	4.50	1.50	1.00	0.00
φ [°]	$-\pi/2$	$-\pi/2$	π	π	$-\pi/2$	$-\pi/2$	$-\pi/2$	$-\pi/2$	$-\pi/2$	0	0

C. Scalability & Wireless Network Requirements

In order to evaluate the viability of the proposed method in practical applications, not only does the accuracy have to be considered, but also the requirements of the real-time data streams on the wireless network deployment. In the given scenario, remote SLAM and wired UWB anchors are used. This means that the video data, here averaging 1.6 Mbit/s, has to be send to the ground control station and the control output at around 25 kbit/s has to be transmitted to the UAV. The above mentioned net data rates were measured by capturing and dissecting the traffic at the IEEE 802.11ac access point. Depending on the application the S-UWB system is used in, the data from the UWB anchors might also be transmitted wirelessly at 26 kbit/s per anchor and mobile node. If cooperative SLAM is desired and the SLAM estimation runs locally on multiple drones, a point cloud of the tracked points needs to be exchanged, assuming a constantly changing environment such as in high-bay storage. The traffic of the point cloud would be and stable manner. Although no reference system is in place, the system is able to maneuver the UAV outside and inside the cage without major deviation from the desired trajectory. To make the results reproducible and provide further material to assess the presented experiments the raw data produced in this work [24] is provided alongside with a video depicting the individual scenarios [25], see Fig. 10.

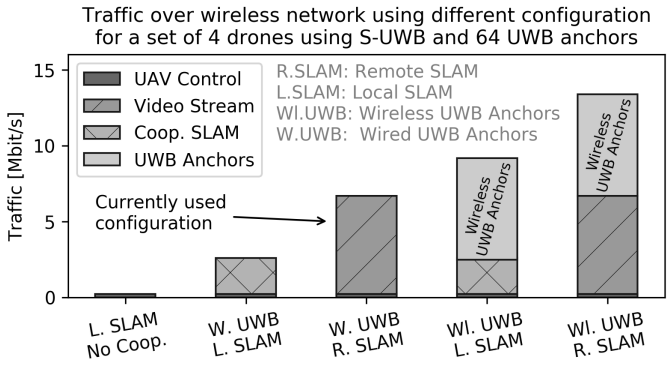

Fig. 11. Comparative bar chart of potential S-UWB configurations and the implications for the resulting real-time traffic load on the wireless network.

around 0.6 Mbit/s for 200 tracked points at 30 Hz. An overview of the net traffic implications for a practical deployment of 4 drones and 64 UWB anchors is depicted in Fig. 11. It is clearly visible that even with a completely wireless approach, the proposed method is viable using modern wireless networks. Nevertheless, the overhead introduced on pre-existing traffic and the potential real-time requirements are note neglectible and have to be subject to future research.

IV. Conclusion and Future Work

This paper proposes a novel approach to enable the seamless use of UAVs in large scale cyber-physical industrial applications. Through augmenting ultra-wideband localization with monocular SLAM, UAV indoor navigation is enabled in areas not covered by wireless localization. Next to a detailed description of the proposed system, an experiment was conducted to evaluate the localization accuracy of different approaches. A second experiment proved the capabilities of the proposed approach outside of the wireless localization coverage. Furthermore, the scalability implications for the proposed approach were analyzed for different configurations. The raw localization results [24] and a video [25] demonstrating the performance of the proposed approach are provided alongside this work. Future work will focus on seamless integration of co-operative SLAM in a multi-UAV testbed, reducing the computational load and continuously improving the positioning with sparsely distributed UWB reference nodes considering inertial sensors and UWB-specific signal quality assessment.

Acknowledgement

The work on this paper has been partially funded by Deutsche Forschungsgemeinschaft (DFG) within the Collaborative Research Center SFB 876 “Providing Information by Resource-Constrained Analysis”, project A4 and was supported by the federal state of Northrhine-Westphalia and the “European Regional Development Fund” (EFRE) 2014-2020 in the course of the “CPS.HUB/NRW” project under grant number EFRE-0400008. The stay of Mr. Ramsey at TU Dortmund was supported by the German Academic Exchange Service (DAAD) in the course of the Research Internships in Science and Engineering (RISE) program.

References

[1] G. Ducard and R. D’Andrea. Autonomous quadrotor flight using a vision system and accommodating frames misalignment. In *IEEE International Symposium on Industrial embedded systems, 2009. SIES’09.*, pages 261–264, 2009.

[2] N. Michael, D. Mellinger, Q. Lindsey, and V. Kumar. The GRASP multiple micro-UAV testbed. *IEEE Robotics Automation Magazine*, 17(3):56–65, Sep 2010.

[3] S. Lupashin, M. Hehn, M. W. Mueller, A. P. Schoellig, M. Sherback, and R. D’Andrea. A platform for aerial robotics research and demonstration: The flying machine arena. *Mechatronics*, 2014.

[4] A. Ledergerber, M. Hamer, and R. D’Andrea. A robot self-localization system using one-way ultra-wideband communication. In *Intelligent Robots and Systems (IROS), 2015 IEEE/RSJ International Conference on*, pages 3131–3137, Sep 2015.

[5] J. Tiemann and C. Wietfeld. Scalable and precise multi-UAV indoor navigation using TDOA-based UWB localization. In *2017 International Conference on Indoor Positioning and Indoor Navigation (IPIN)*, Sapporo, Japan, Sep 2017.

[6] S. Mafrica, A. Servel, and F. Ruffier. Minimalistic optic flow sensors applied to indoor and outdoor visual guidance and odometry on a car-like robot. *Bioinspiration and Biomimetics*, 11(6):066007, 2016.

[7] D. Hoeller, A. Ledergerber, and R. D’Andrea. Augementing ultra-wideband localization with computer vision for accurate flight. In *Proceedings of the World Congress of the International Federation of Automatic Control*, to appear 2017.

[8] H. Johannsson, M. Kaess, M. Fallon, and J. J. Leonard. Temporally scalable visual SLAM using a reduced pose graph. In *2013 IEEE International Conference on Robotics and Automation*, pages 54–61, May 2013.

[9] A. Bry, A. Bachrach, and N. Roy. State estimation for aggressive flight in GPS-denied environments using onboard sensing. In *2012 IEEE International Conference on Robotics and Automation*, pages 1–8, May 2012.

[10] C. Wang, K. Li, G. Liang, H. Chen, S. Huang, and X. Wu. A heterogeneous sensing system-based method for unmanned aerial vehicle indoor positioning. *Sensors*, 17(8), 2017.

[11] F. J. Perez-Grau, F. Caballero, L. Merino, and A. Viguria. Multi-modal Mapping and Localization of Unmanned Aerial Robots based on Ultra-Wideband and RGB-D sensing. In *Intelligent Robots and Systems (IROS), 2017 IEEE/RSJ International Conference on*, Sep 2017.

[12] E. B. Quist and R. W. Beard. Radar odometry on fixed-wing small unmanned aircraft. *IEEE Transactions on Aerospace and Electronic Systems*, 52(1):396–410, February 2016.

[13] F. Fraundorfer, L. Heng, D. Honegger, G. H. Lee, L. Meier, P. Tanskanen, and M. Pollefeys. Vision-based autonomous mapping and exploration using a quadrotor MAV. In *2012 IEEE/RSJ International Conference on Intelligent Robots and Systems*, pages 4557–4564, Oct 2012.

[14] L. von Stumberg, V. C. Usenko, J. Engel, J. Stückler, and D. Cremers. Autonomous exploration with a low-cost quadrocopter using semi-dense monocular SLAM. *CoRR*, abs/1609.07835, 2016.

[15] D. Gehrig, M. Goettgens, B. Paden, and E. Frazzoli. Scale-corrected monocular-SLAM for the AR.Drone 2.0. 2017. Preprint.

[16] R. Huang, P. Tan, and B. M. Chen. Monocular vision-based autonomous navigation system on a toy quadcopter in unknown environments. In *2015 International Conference on Unmanned Aircraft Systems (ICUAS)*, pages 1260–1269, June 2015.

[17] O. Esrafilian and H. D. Taghirad. Autonomous flight and obstacle avoidance of a quadrotor by monocular SLAM. In *2016 4th International Conference on Robotics and Mechatronics (ICROM)*, pages 240–245, Oct 2016.

[18] E. Lopez, S. Garca, R. Barea, L. M. Bergasa, E. J. Molinos, R. Arroyo, E. Romera, and S. Pardo. A multi-sensorial simultaneous localization and mapping (SLAM) system for low-cost micro aerial vehicles in GPS-denied environments. *Sensors*, 17(4), 2017.

[19] M. Quigley, K. Conley, B. P. Gerkey, J. Faust, T. Foote, J. Leibs, R. Wheeler, and A. Y. Ng. ROS: an open-source robot operating system. In *ICRA Workshop on Open Source Software*, 2009.

[20] M. Monajjemi, S. Mohaimenianpour, and R. Vaughan. UAV, come to me: End-to-end, multi-scale situated HRI with an uninstrumented human and a distant UAV. In *Intelligent Robots and Systems (IROS), 2016 IEEE/RSJ International Conference on*, pages 4410–4417, 2016.

[21] R. Mur-Artal, J. M. M. Montiel, and J. D. Tardós. ORB-SLAM: a versatile and accurate monocular SLAM system. *IEEE Transactions on Robotics*, 31(5):1147–1163, Oct 2015.

[22] R. Mur-Artal and J. D. Tardós. ORB-SLAM2: an open-source SLAM system for monocular, stereo and RGB-D cameras. *IEEE Transactions on Robotics*, 33(5):1255–1262, 2017.

[23] J. Tiemann, F. Eckermann, and C. Wietfeld. ATLAS - an open-source TDOA-based ultra-wideband localization system. In *2016 International Conference on Indoor Positioning and Indoor Navigation (IPIN)*, Alcalá de Henares, Madrid, Spain, Oct 2016.

[24] J. Tiemann and A. Ramsey. Raw experimental data, http://dx.doi.org/10.5281/zenodo.888104. Dec 2017.

[25] J. Tiemann, A. Ramsey, and O. Nguyen. Enhanced UAV indoor navigation through SLAM-augmented UWB localization, video: https://vimeo.com/232110091. 2017.